Thermal-hydraulic performance of oval tubes in a cross-flow of air

ALA HASAN

Helsinki University of Technology, Laboratory of Heating, Ventilating and Air Conditioning, P. O. Box 4400, FIN-02015 HUT, Finland

E-mail: ala.hasan@hut.fi
Tel.: + 358 9 4513598;
fax: + 358 9 4513418.

Abstract

The thermal-hydraulic performance of five oval tubes is experimentally investigated and compared with that for a circular tube in a cross-flow of air. The range of Reynolds numbers Re_D is approximately between 1000 and 11000. The nominal axis ratios R (major axis / minor axis) for three of the investigated oval tubes are 2, 3, and 4. Two other configurations of oval tubes are also tested, an oval tube R = 3 with two wires soldered on its upper and lower top positions, and a cut-oval tube. The performance of the tubes is corrected for the effects of area blockage and turbulence intensity.

The measurement results show that the mean Nusselt numbers Nu_D for the oval tubes are close to that for the circular tube for Re_D < 4000. For a higher Re_D, the Nu_D for the oval tubes is lower than that for the circular tube and it decreases with the increase in the axis ratio R. The drag coefficients C_d for the tubes are measured and the combined thermal-hydraulic performance is indicated by the ratio Nu_D / C_d, which shows a better combined performance for the oval tubes.

Keywords: heat transfer; drag coefficient; oval; circular; tube

List of Symbols

A_i, A_o	internal, external area of a tube, (m^2)
A_F	frontal area of a tube, (m^2)
c	outer major axis or chord, (m)
C_d	drag coefficient, $C_d = F_d / (0.5\, \rho\, V_T^2 A_F)$
$C_{d\ avg}$	average drag coefficient
D	diameter, (m)
D_o	for a circular tube: outside diameter, for an oval tube: outside diameter of a circular tube having equivalent perimeter, (m)
F_d	drag force, (N)
k_a	thermal conductivity of air, ($W\ m^{-1}\ K^{-1}$)
k_w	thermal conductivity of wall, ($W\ m^{-1}\ K^{-1}$)
Nu	Nusselt number, $Nu = \alpha_a D / k_a$
Nu_D	mean Nusselt number for a tube, $Nu_D = \alpha_a D_o / k_a$
R	nominal axis ratio for an oval tube (major axis / minor axis)
Re	Reynolds number, $Re = V D \rho / \mu$
Re_c	Reynolds number, $Re_c = V_T\, c\, \rho / \mu$
Re_D	Reynolds number, $Re_D = V_f D_o \rho / \mu$
V	air velocity, ($m\ s^{-1}$)
V_f	free stream velocity of air, ($m\ s^{-1}$)
V_T	upstream velocity of air to the test section, ($m\ s^{-1}$)
y	outer minor axis of an oval tube, (m)
α_a	air-side convective heat transfer coefficient, ($W\ m^{-2}\ K^{-1}$)
α_H	water-side convective heat transfer coefficient, ($W\ m^{-2}\ K^{-1}$)
Δt_{lm}	log-mean-temperature-difference, (°C)

1. Introduction

Oval tubes in a cross-flow of air exhibit lower air pressure drop than circular tubes. The operating costs in cross-flow heat exchangers are mainly due to the energy required to move air across the tubes. While the advantage gained from their hydraulic performance is clear, the thermal performance of oval tubes is not well agreed upon.

Maybe the oldest work on a single elliptical cylinder mentioned in the literature is that by Reiher in 1925 [1], as quoted by Ota et al. [2], who reported the mean heat transfer coefficient for an elliptical cylinder whose configuration was obscure. Ota et al. [2] investigated experimentally the thermal performance of a single elliptical cylinder with an axis ratio (major axis to minor axis) of 2 in a flow of air having Reynolds numbers (Re_c) of 5000 to 90000 with angles of attack from 0 to 90˚ (where Re_c is the Reynolds number based on the major axis c). For air flow parallel to the major axis, they found that the Nusselt number for the elliptical cylinder was higher than that obtained for a circular cylinder from an empirical correlation by Hilpert [3]. Ota et al. [4] tested an elliptical cylinder with an axis ratio of 3 with Re_c from 8000 to 79000. The Nusselt number for the elliptical cylinder was found to be higher than that for a circular cylinder from Hilpert's correlation. When they compared the results of their measurements with those for the elliptical cylinder with an axis ratio of 2 mentioned in [2], a small increase in heat transfer was noticed. Kondjoyan and Daudin [5] studied experimentally the effect of variation in the free stream turbulence intensity Tu from 1.5% to 40% on the heat transfer from a circular cylinder and an elliptical cylinder (axis ratio 4) for Reynolds numbers Re_D between 3000 and 40000 (Re_D is based on the diameter of the equivalent circular cylinder for an elliptical cylinder). Their conclusion was that turbulence intensity effect is as important as air velocity effect. They indicated that the Nusselt number for the elliptical cylinder was about 14% lower than that for the equivalent circular cylinder.

For flow around an elliptical cylinder, Schubauer [6] made measurements of the velocity distribution inside the laminar boundary layer, and Hoerner [7] showed the drag coefficient as a function of the axis ratio.

For more than one tube or for a bank of tubes, Merker and Hanke [8] found experimentally the heat transfer and pressure drop performance of staggered oval tube banks with different transversal and longitudinal spacings. The oval tube axis ratio was 3.97. They showed that an exchanger with oval-shaped tubes had smaller frontal areas on the shell-side compared to those with circular tubes. Ota and Nishiyama [9] investigated experimentally the flow around two elliptical cylinders (axis ratio 3) which were in a tandem arrangement. The static pressure distribution on the surface was measured and the drag, lift, and moment coefficients were evaluated for a range of angles of attack and cylinder spacings. Nishiyama et al. [10] investigated the heat transfer around four elliptical cylinders (axis ratio 2) which were placed in a tandem arrangement in air with Reynolds numbers Re_c from 15000 to 70000. They showed that the thermal performance of the elliptical cylinders was comparable to that of in-line circular cylinders at narrower cylinder spacings and at smaller angles of attack. Salazar et al. [11] measured the heat transfer from a bank of elliptical tubes in a cross-flow. The elliptical tube axis ratios used were 1.054, 1.26, and 1.44. The characteristic length in Re and Nu for the elliptical tube was assumed to be equal to the minor axis. The results indicated that correlations of circular tubes were slightly higher than the measurements of the elliptical tubes. Liu et al. [12] examined experimentally the performance of an array of 18 elliptical tubes, where the tube axis ratio was 3.33. In their work, the colder tube array cooled warmer air which flowed normal to the tubes. They evaluated the Nusselt number and the dimensionless pressure drop factor on the air side.

For finned elliptical tubes there are several experimental works, Brauer [13] and Schulenberg [14] showed better heat transfer for finned elliptical tubes than for finned circular tubes, and Saboya and Saboya [15] indicated no major differences, while Jang and Yang [16] indicated lower heat transfer performance for finned elliptical tubes.

For evaporatively cooled heat exchangers, Hasan and Sirén [17] showed that a bank of wet oval tubes has a better combined thermal-hydraulic performance than corresponding circular tubes.

No special conclusions could be drawn from the available literature concerning the expected thermal performance of oval tubes relative to circular tubes. While some works in the literature refer to better thermal performance, others indicate the reverse.

The objective of the current work is to investigate experimentally the performance of oval tubes in a cross-flow of air in the low Reynolds number range (approximately $1000 < Re_D <$

11000) and to compare the performance with that for an equivalent circular tube. Oval tubes of five shapes will be investigated: oval tubes with three nominal axis ratios (R = 2, 3, and 4), and two other tube configurations; one is an oval tube R = 3 which has two wires soldered on its upper and lower surfaces, and the other one is a cut-oval tube. The feasibility of using oval tubes in heat transfer will be presented in terms of their combined thermal-hydraulic performance.

2. Tube dimensions

A special tool (Fig. 1 (a)) was manufactured by the Laboratory of Production Engineering-Helsinki University of Technology to form the oval tubes from soft circular copper tubes. The tool is composed of three rollers; one is a guiding roller and two are active rollers. To form an oval tube, a channel possessing the shape of half of the required oval tube was machined on the two opposite surfaces of the active rollers. The circular tube was placed into the cavity between the two rollers, pressed by the rollers, and pulled out to form an oval tube.

Five oval tube shapes are investigated in this work. The dimensions of the tubes are indicated in Fig. 1 (b). The axis ratios (outer major axis c to outer minor axis y) for three of the oval tubes are 1.9, 2.8, and 4, which will be referred to by nominal values of R = 2, 3, and 4, respectively. Additionally, the investigation covers two other tube configurations. One is an oval tube R = 3 with two steel wires soldered along the tube at a central angular position of ± 90°. The wire cross-section is semicircular and its height is 1 mm. The profile of the second tube is composed of two identical arcs of a bigger oval shape which is cut at a right angle at the rear. This tube will be referred to as the cut-oval tube. Its minor axis is equal to that for the oval tube R = 3, and its major axis is shorter (c = 23.3 mm). This tube was formed by the same method used for the other oval tubes.

The perimeter of the formed tubes was made equal to that of the circular tube (D_o = 18 mm) from which they were formed. This means that the heat transfer area is equal for all of the investigated tubes.

3. Test rigs

3.1. Test rig for the thermal measurements

A test rig was built for the measurement of heat transfer from the tubes in a cross-flow of air. The test rig includes a wind tunnel, test section, water system, fan, and measuring instruments. Fig. 2 shows the basic components of the test rig. Air was driven through the wind tunnel and test section by a fan under an induced draft. A frequency converter was used to control the rotational speed of the fan. The flow rate of the air was measured by a pressure difference measuring device. Heat transfer took place in the test section from hot water flowing inside the tubes to air in a cross-flow. The hot water was circulated in the water system. Thermocouples type T were used for the measurement of the air and hot water temperatures. They were mounted at the inlet and outlet of the test section, at the air side and water side.

Wind tunnel

A low-speed wind tunnel was built to provide uniform air velocity distribution in the test section. The wind tunnel length is 1500 mm. The wind tunnel inlet and outlet are square, with dimensions of 800 mm × 800 mm and 400 mm × 400 mm, respectively. The area contraction ratio is four, which is in accordance with values mentioned by Pankhurst and Holder [18]. The profile of the wind tunnel is a sixth-order polynomial, which was designed according to Lassila [19].

Water system

The water system comprises an electric heater, pump, water flow meter, electric power meter, and thermocouples. The tube, which is made of copper, makes four passes through the test section. The water system is insulated from the surroundings. The electric heater was used to increase the water temperature so that the inlet water temperature to the test section was kept at about 70ºC. The pump circulated the hot water inside the tube in a closed circuit. Heat transfer took place from the hot water to the air which flowed normally to the tubes. The electric power meter was used to measure the power supply to the water system. The relatively high inlet water temperature and the multiple tube passes result in a higher rate of heat transfer, which would decrease measurement errors.

Test section

The cross-sectional dimensions of the test section are 400 mm × 400 mm. The four passes of the tube constitute a single array of tubes in the test section and as shown by Fig. 3 (a) and (b). The horizontal length of each pass in the test section is 400 mm. The circular tube outside diameter D_o is 18 mm. The transversal tube spacing is 80 mm which is 4.45 D_o. For a single array of tubes, as in the current work, Zukauskas [20] indicated that the heat transfer from one tube in the array is similar to that for a single tube standing alone in the test section.

The existence of a tube in a channel and the related effect of flow restriction (Fig. 3 (c)) will be taken into consideration by the blockage effect in Section 4.1.1.
The air velocity in an empty test section was approximately from 1 to 10.5 m s^{-1}, which covers a wide range for general heat transfer applications. The Reynolds number Re_D, based on the aforementioned air velocity values and the tube diameter, is approximately from 1000 to 11000. This is in the lower range of the subcritical external flow.
The surfaces of the tubes were polished to eliminate radiation heat transfer. A bright tube has an emissivity of 0.02, which makes its radiation losses negligible.

3.2. Test rig for the hydraulic measurements

The hydraulic behaviour of the tubes will be found from the drag force measurements. A simple method was used to find the drag coefficient C_d for the tubes and as shown by Fig. 4. The tube was placed in the horizontal axis of the test section. It filled the test section and extended outside the side walls through two holes, where it was connected from its ends by two arms to an accurate electronic weighing scale. There is a small tolerance between the surface of the tube and the edges of the two holes. One tube was investigated each time. When there is no air flow, the freely suspended tube is in its reference position, where its major axis is at right angles to the vertical axis of the test section. When air flows in the test section, the tube moves from its reference position. The drag force is determined from the force required to mantain the tube in its reference position.

4. Experimental measurements

The overall characteristics of the tubes will be determined from the thermal and hydraulic measurements. Prior to that, the following preparation measurements were carried out:

Measurements of air velocity distribution at wind tunnel outlet

Air velocity was measured at the wind tunnel outlet using a pitot-static tube for a velocity range of approximately 1 to 17 m s^{-1}. The measurements were taken along the vertical and the horizontal centrelines of the wind tunnel outlet. Fig. 5 shows a typical velocity distribution from the measurement. As seen, the wall effect is confined to a narrow region adjacent to the wall and the velocity distribution at the positions of the tubes is uniform.

Measurements of heat loss from the insulation

The hot water system (components and piping) was insulated from the surroundings. Heat loss through the insulation to the surroundings was measured by shortcutting the water system which was done by bypassing the tubes inside the test section and operating the hot water system. The insulation resistance for heat loss to the surroundings was found by measuring the electrical power supply required to keep a steady state temperature for the water. The importance of this could be recognised if we know that the results of the thermal measurement for the tubes, which will be presented next, would show that the ratio of the heat loss through the insulation to the total heat supplied to the hot water was between 10 to 34%.

4.1. Thermal measurements

The amount of heat transfer q from hot water to air for a circular tube is governed by the equation

$$q = \frac{\Delta t_{\mathrm{lm}}}{\dfrac{1}{\alpha_{\mathrm{a}}\, A_{\mathrm{o}}} + \dfrac{D_{\mathrm{o}}}{2\, k_{\mathrm{w}} A_{\mathrm{o}}} \ln\left(\dfrac{A_{\mathrm{o}}}{A_{\mathrm{i}}}\right) + \dfrac{1}{\alpha_{\mathrm{H}}\, A_{\mathrm{i}}}} \quad (1)$$

where Δt_{lm} is the log-mean-temperature-difference between the hot water and cross-flow air temperatures. The internal convective heat transfer coefficient for the hot water α_{H} can be calculated using the Gnielinski correlation from [21]. The tube wall thermal resistance to heat conduction and the internal flow resistance to heat convection are too small (together <1% of the total thermal resistance), so that the resistance to convective heat transfer from the tube surface to air ($1 / \alpha_{\mathrm{a}} A_{\mathrm{o}}$) dominates. For a steady state case, the amount of heat transfer from hot water to air q is evaluated from the measured electrical power supply, which is converted into heat, and the insulation heat loss. This method is more accurate than evaluating q from the measurement of the small temperature drop of water in the test section. The temperature difference Δt_{lm} is determined from the temperature measurements for air and water. Therefore, the air-side convective heat transfer coefficient for the tube α_{a} can be found from Eq. (1), from which the mean Nusselt number for the tube ($\mathrm{Nu}_{\mathrm{D}} = \alpha_{\mathrm{a}} D_{\mathrm{o}} / k_{\mathrm{a}}$) can be evaluated. The highest value of ($\mathrm{Gr} / \mathrm{Re}_{\mathrm{D}}^{2}$) for air in this work was about 0.025 (where Gr is the Grashof number). Since this value is <<1, then the effect of the natural convection could be neglected according to [21]. The thermophysical properties of the air are evaluated at the average temperature between air and hot water temperatures.

4.1.1. Heat transfer measurements for the circular tube

Heat transfer measurements were carried out for the circular tube, where the 18 mm o. d. circular tube is considered as a reference case for the measurements. Morgan [22] reviewed more than 100 references for the relation between the Nusselt number Nu_D and the Reynolds number Re_D for a circular cylinder in a cross-flow of air. He proposed heat transfer correlations in the form $\mathrm{Nu}_\mathrm{D} = n_1 \,\mathrm{Re}_\mathrm{D}^{\,n_2}$, where in his correlations, Nu_D is for turbulence free flow and Re_D is defined in terms of the air free stream velocity V_f. Morgan indicated in [22] that his proposed correlations are the same as Hilpert's [3] when the latter are corrected by using modern data for the thermophysical properties of air.
The results of heat transfer measurements for the circular tube in the current work will be compared to Morgan's correlations. The characteristics of the tubes will be corrected for the blockage effect (solid and wake blockages) and the turbulence effect.

Solid and wake blockages effect

This effect is due to the flow obstruction produced by placing a tube in a channel, which will increase the free stream velocity V_f, as shown by Fig. 3 (c). To correct for the solid and wake blockages effect for a circular cylinder, Morgan [22] used a correction equation by Vincenti and Graham [23], who used the method of superposition to account for these effects for a closed-throat wind tunnel of diameter D_T

$$V_\mathrm{f} = V_\mathrm{T}\left[1 + 0.321 C_\mathrm{d} (D / D_\mathrm{T}) + 1.356 \,(D / D_\mathrm{T})^2\right] \qquad (2)$$

where V_f is the free stream velocity of the obstructed flow, V_T is the upstream velocity of air to the test section, C_d is the drag coefficient, and D is the outside diameter of the tube. Eq. (2) will be implemented for the correction of this effect in the current work. D is taken as D_o for the circular tube or y (the outer minor axis) for the oval tubes. D_T is taken as the height of the flow channel per one tube. Values of C_d are substituted in Eq. (2) as they are found from the hydraulic measurements (Section 4.2). For the data from the current work, Eq. (2) shows that $V_f / V_T = 1.1$ for the circular tube, and $V_f / V_T \leq 1.04$ for the oval tubes.

Turbulence intensity effects

The turbulence intensity Tu is defined as the root mean square of the instantaneous velocity deviations from the value of the mean velocity, divided by the mean velocity ($\mathrm{Tu} = \frac{\sqrt{\overline{V'^2}}}{\overline{V}}$ where V' is the instantaneous deviations from the mean air velocity $\overline{V}$).

Free stream turbulence intensity produced by instantaneous fluctuations of air velocity at the test-section was measured by means of a hot-wire anemometer. These measurements indicated that the turbulence intensity was from 0.7% to 3.8% for air velocity from 1.1 to 10.8 m s^{-1}, respectively. The effect of higher free stream turbulence intensity is higher heat transfer rate from the tube surface. Correlations presented by Comings et al. [24] and van der Hegge Zijnen [25] were considered by Morgan [22] to evaluate the increase in the Nusselt number ΔNu_D due to the turbulence intensity in the direction of flow for circular cylinders in the range of Re_D = 10000 and as the following

$$\frac{\Delta \mathrm{Nu_D}}{\mathrm{Nu_D}} = 1.29\sqrt{\mathrm{Tu}} \quad \text{for } 1\% \leq \mathrm{Tu} < 3\%, \qquad (3a)$$

$$\frac{\Delta \mathrm{Nu_D}}{\mathrm{Nu_D}} = 2.42\ \mathrm{Tu}^{2/3} \quad \text{for } 3\% \leq \mathrm{Tu} \leq 12\%\,. \qquad (3b)$$

This equation will be considered to correct for the turbulence effect in the current work. For the flow turbulence intensity in this work (Tu = 0.7% to 3.8%), Eq. (3) shows 11% to 27% increase in Nu_D.

Checking the circular tube measurements

Fig. 6 shows the measurement results for the 18 mm o. d. circular tube. The correction equations, Eqs. (2) and (3), are implemented to correct for the blockage effect and the turbulence effect, respectively. For the blockage effect, the measurement points, which are presented in terms of the Reynolds number based on V_T, are shifted towards higher values based on V_f. The effect of the turbulence intensity on the heat transfer is excluded which results in lower Nu_D. The final measurement points after the corrections are shown with their error bars in Fig. 6 relative to Morgan's correlation [22], who indicated that his correlation involves a maximum uncertainty of ± 5%. As seen in the figure, the corrected measurements points are very close to the correlation. This is a check of the measuring procedure and facilities.

4.1.2. Heat transfer measurements for the oval tubes

The major axis of the oval tubes was parallel to the direction of the air flow. The oval tubes were formed from 18 mm o.d. copper circular tubes, which after forming preserved the same perimeter as the circular tube. When the performance of the oval tubes is compared with that for the circular tube, it will be on the basis of the utilisation of the same surface area. Therefore, for the same air velocity, any difference in the characteristics will result from the different surface geometry (oval or circular).

The thermal performance of the circular tube and three oval tubes (having nominal axis ratios R of 2, 3, and 4) is shown in Fig. 7. The measurement results are corrected for the effects of area blockage and flow turbulence as per Eqs. (2) and (3), respectively. To compare with the circular tube, the characteristic length in the definition of the Reynolds and Nusselt numbers for the oval tubes is taken to equal the outside diameter of the circular tube which has the equivalent perimeter (here D_o = 18 mm), and will be written as Re_D and Nu_D, respectively. This definition was implemented by Ota et al. [2, 4] and Kondjoyan and Daudin [5]. A similar definition for noncircular tubes was indicated by Jacob [26].

It appears that for lower Reynolds numbers in Fig. 7 (Re_D < 4000), the differences between Nu_D for the circular and oval tubes are small that almost all of the measurement points for the oval tubes are within a ± 5% range around the measurement points for the circular tube. Note that Re_D < 4000 here corresponds to an air velocity of less than 4 m s^{-1}, which is the range for most air-conditioning applications. Beyond this velocity, Nu_D for the oval tubes is lower than that for the circular tube and it decreases with the increase of the axis ratio R. At Re_D = 11000, the decrease in Nu_D for the oval tubes from that for the circular tube is 8% for R = 2 and 16% for R = 3 and R = 4. Kondjoyan and Daudin [5] also reported lower Nu_D for an elliptical cylinder having R = 4 compared with that for an equivalent circular cylinder.

For subcritical flow around a circular tube, separation of the laminar boundary layer occurs at an angle of about 80º due to the expansion in flow area and the adverse pressure gradient. The local Nu is largest at the stagnation point and decreases with the distance along the surface due to the growth of boundary layer thickness. The local Nu reaches its minimum near the separation point. Beyond that, the local Nu increases because considerable turbulence exists where the eddies of the wake affect the surface. The local Nu over the rear-side of the circular tube is smaller than that for the stagnation point because fluid recirculation is not effective in mixing the fluid in the vicinity of the surface with the fluid in the main stream. A similar behaviour exists for oval tubes. For the location of the separation point of elliptical tubes, Ota. et al. [2] stated that separation occurred at $s / c = 0.6$ for $R = 2$ which almost coincided with the location of the minor axis, and Ota et al. [4] stated that it occurred at $s / c = 0.7$ for $R = 3$ which was a little downstream of the location of the minor axis, where s is the distance on the tube surface. Schubauer [6] indicated that for $R = 2.96$ separation happened at an angle of approximately 120º, and Kondjoyan and Daudin [5] showed it at approximately 105º for $R = 4$.

Generally, it is noted that the coefficients of the empirical correlations for heat transfer for a circular tube change for some ranges of Re_D. For the range relevant to the current work, it is noted that Morgan's correlations and Hilpert's corrected correlations in [22] show that the coefficients change at $Re_D = 5000$. This would mean that the heat characteristics of the tube start to change at the indicated Re_D value. This could have a relation to the behaviour noticed in our measurements, where the discrepancies between the oval and circular tubes increased for $Re_D > 5000$.

For external flow around an object, the boundary layer grows thicker as the surface becomes flatter. This explains the decrease of Nu_D for the oval tubes for $Re_D > 4000$. The change of the tube geometry from circular to oval for $Re_D < 4000$ seems to have an insignificant effect on the thermal behaviour. Correlation equations fitted to the data presented in Fig. 7 indicate that $Nu_D = 0.728\ Re_D^{0.437}$ for all the points which have $Re_D \leq 4000$, while for the points with $4000 < Re_D \leq 11000$: $Nu_D = 0.117\ Re_D^{0.656}$ for the circular tube, $Nu_D = 0.209\ Re_D^{0.583}$ for the oval tube $R = 2$, and $Nu_D = 0.357\ Re_D^{0.517}$ for the oval tubes $R = 3$ and $R = 4$.

Two other tube configurations were also investigated, the cut-oval tube and the oval tube $R = 3$ with the two wires. For the latter tube, the diameter of the equivalent circular tube includes also the wetted perimeter of the wires. The location of the wire is a little upstream of the expected separation point for a plain oval tube. Fig. 8 shows Nu_D and Re_D for these two tubes together with that for the oval tube R = 3. The tubes indicated in Fig. 8 seem to have almost identical thermal performance.

4.2. Hydraulic measurements

The drag coefficient C_d for each tube is found from the measurements of the drag force F_d. The latter consists of the skin friction force on the tube surface and the form drag due to separation at the rear-side of the tube, both of which are affected by the shape of the tube. The pressure drop of the air flow across the tube is related to C_d. The drag coefficient is

$$C_d = \frac{F_d}{0.5\,\rho\,V_T^{\;2}\;A_F} \qquad (4)$$

where A_F is the tube frontal area which is perpendicular to the free stream direction and ρ is the air density.

The drag measurements for the tubes are presented in Fig. 9 against Re_c which is based on the tube chord (the major axis for the oval tubes) where $Re_c = V_T\, c\, \rho\, /\, \mu$. It can be seen that C_d for the oval tubes is lower than that for the circular tube, and it decreases with increased oval tube axis ratio. C_d for the cut-oval tube is lower than that for the oval having R = 3, while the addition of the wires on the latter tube increases its C_d. Table 1 shows the average values of the drag coefficient $C_{d\,avg}$ for the tubes together with that available from the literature for comparable sections. The data for the elliptical sections are taken from Hoerner [7] for subcritical flow. For the circular tube, the measured $C_{d\,avg}$ is 1.05, while Morgan [22] indicated that $C_{d\,avg} \approx 1.2$ (for $10^2 \leq Re_D \leq 10^5$, tube aspect ratio > 10, blockage ratio << 1, and Tu <<1), and Knudsen and Katz [27] indicated that $C_{d\,avg} = 1.0$ for $10^4 \leq Re_D \leq 2 \times 10^5$.

4.3. Combined thermal-hydraulic performance of the tubes

The ratio of the Nusselt number to the drag coefficient ($Nu_D / C_{d\,avg}$) is taken as an indication of the thermal-hydraulic characteristics of the tubes. To compare the performance at the same air velocity, $Nu_D / C_{d\,avg}$ would refer to the amount of heat transfer from a tube to the energy required to move the air across the tube. Fig. 10 shows $Nu_D / C_{d\,avg}$ for the tubes as determined from the measurement data. It can be seen from this figure that the oval tubes are better than the circular tube in a combined thermal-hydraulic performance. The ratio of $\mathrm{Nu_D} / C_{\mathrm{d\,avg}}$ for each oval tube to that for the circular tube $\dfrac{(\mathrm{Nu_D}/C_{\mathrm{d\,avg}})_{\mathrm{oval}}}{(\mathrm{Nu_D}/C_{\mathrm{d\,avg}})_{\mathrm{circular}}}$ has the average values indicated by Table 2 for the investigated range of $\mathrm{Re_D}$. These values indicate better combined thermal-hydraulic performance for the tested oval tubes compared with that for the circular tube.

4.4. Analysis of the measurement errors

To find the uncertainty in the measurements of a final variable f (e.g. Nu, Re, C_d), error analysis is performed using the accuracy in the readings of independent variables x_i (e.g. temperature, power, tube dimension, thermophysical property, pressure difference, force). Errors in the measurements of the independent variables dx_i propagates in the calculation of the uncertainty of the dependent variable df according to

$$\mathrm{d}f = \sqrt{(\frac{\partial f}{\partial x_1}\mathrm{d}x_1)^2 + (\frac{\partial f}{\partial x_2}\mathrm{d}x_2)^2 + (\frac{\partial f}{\partial x_3}\mathrm{d}x_3)^2 + ...} \quad (5)$$

For the temperature measurements: The thermocouples were connected to a data-logger which has an accuracy of ± (0.1% of reading + 0.2 % of range span). The logger readings were calibrated against readings of a mercury-in-glass thermometer. The accuracy of this thermometer is taken equal to ± 0.01 $^{\circ}$C which is one-half its smallest scale division. The error in the temperature measurement is due to the logger error, the residual of the systematic error after calibration, and the thermometer error. Then the uncertainties in the water and air temperature readings are 0.92 $^{\circ}$C and 0.83 $^{\circ}$C, respectively.

For the power measurements: The power meter readings were calibrated against a reference multimeter. The above-mentioned logger registers also the power readings. The power measurement error includes the logger error, the residual of the error after calibration, and the reference multimeter error.

For the tubes dimensions: A digital calliper was used, which has an accuracy of ± 0.00003 m. For the measurement of lengths, 0.0005 m is taken as one-half of the smallest scale division of the used tape measure.

The error in the thermophysical properties of air (kinematic viscosity, thermal conductivity, and density) is taken to correspond to the expected error in the air temperature measurement.

The relative uncertainty is defined as the uncertainty divided by the value of the variable (d*f* / *f*). Therefore the relative uncertainty in Nu_D is found to be between 3.3 and 5.5%, which is approximately equal to the uncertainty in the readings of the electric power meter used for the heat supply measurements.

For the uncertainties in the Reynolds number: The air velocity was determined from pressure difference readings of a micromanometer which was connected to a cross-type volumetric flowmeter. The maximum relative uncertainty in the values of Re_D is found to be 2.7 to 5.6%.

For the uncertainty in the measurements of the drag coefficient Cd: The drag force was measured by a digital weighing scale which has an accuracy of ± 0.05 g. The relative uncertainty in Cd is 2.7 to 7.9%.

Error bars are indicated on figures (6,7, 9, and 10) for the measurements of the circular tube as a typical set of measurements.

5. Conclusions

At the lower range of the investigated Reynolds numbers ($Re_D < 4000$), Nu_D for the oval tubes are close to that for the circular tube, as it seems that the change in the geometry of the tube at this low range of Re_D has only a small effect on the mean heat transfer coefficient. This range of Re_D corresponds to air velocities < 4 m s^{-1} in this work, which is the range for most air-conditioning applications. For a higher Re_D, the Nu_D for the oval tubes is lower than that for the circular tube and it decreases with the increase in the axis ratio R. The decrease in Nu_D for the oval tubes from that for the circular tube at $Re_D = 11000$ is 8% for $R = 2$ and 16% for $R = 3$ and $R = 4$.

Due to the slender shape of the oval tubes, their drag coefficients C_d are lower than that for the circular tube. The investigated oval tubes appeared to have a better combined thermal-hydraulic performance compared with that for the circular tube: the average value of the ratio

$\frac{(\mathrm{Nu}_\mathrm{D}\,/\,C_{\mathrm{d\,avg}})_{\mathrm{oval}}}{(\mathrm{Nu}_\mathrm{D}\,/\,C_{\mathrm{d\,avg}})_{\mathrm{circular}}}$ is 1.6 for R = 2, 1.8 for R = 3, 2.5 for R = 4, 1.3 for the oval tube with the wires, and 2.1 for the cut-oval tube.

These results for single tubes are indicative of the expected performance of bundles of oval tubes, which could be useful to investigate in the future. Because of their smaller face area, oval tube heat exchangers are more compact than circular tube heat exchangers. This means that more oval tubes can be put into a specified volume, which means higher heat transfer area. Added to their better combined thermal-hydraulic performance, this would indicate encouraging characteristics for using oval tubes in heat exchangers.

6. Acknowledgements

The author would like to thank Prof. Kai Sirén for his supervision of this study. The project was funded by the Finnish National Technology Agency (TEKES), Cetetherm Oy, Ekocoil Oy, and Koja Oy.

7. References

[1] H. Reiher, Handbuch der Experimental Physik, Vol. 9, pt. 1, Leipzig, (1925), 312.

[2] T. Ota, S. Aiba, T. Tsuruta and M. Kaga, Forced Convection Heat Transfer from an Elliptic Cylinder of Axis Ratio 1:2, Bulletin of JSME, 26 (212) (1983) 262–267.

[3] R. Hilpert, Forschung Gebiete Ingenierwes, 4 (1933) 215–224.

[4] T. Ota, H. Nishiyama, Y. Taoka, Heat transfer and flow around an elliptic cylinder, International Journal of Heat and Mass Transfer, 27 (10) (1984) 1771–1779.

[5] A. Kondjoyan, J. D. Daudin, Effects of free stream turbulence intensity on heat and mass transfer at the surface of a circular cylinder and an elliptical cylinder axis ratio 4, International Journal of Heat and Mass Transfer, 38 (10) (1995) 1735–1749.

[6] G. B. Schubauer, Air flow in a separating laminar boundary layer, NACA report No. 527. (1936).

[7] F. S. Hoerner, Fluid Dynamic Drag, (1965).

[8] G. P. Merker, H. Hanke, Heat transfer and pressure drop on the shell-side of tube-banks having oval-shaped tubes. International Journal of Heat and Mass Transfer, 29 (12) (1986) 1903–1909.

[9] T. Ota, H. Nishiyama, Flow around two elliptic cylinders in tandem arrangement, Journal of Fluids Engineering, Transactions of the ASME, 108 (1) (1986) 98–103.

[10] H. Nishiyama, T. Ota, T. Matsuno, Forced convection heat transfer from elliptic cylinders in tandem arrangement. Proceedings of the 1987 ASME-JSME Thermal Engineering Joint Conference, Honolulu, HI, USA, 4 (1987), 151–157.

[11] E. Salazar, J. J. Gonzalez, A. Lopez De Ramos, F. Pironti, D. Gonzalez-Mendizabal, Evaluation of the heat transfer coefficient in a bank of elliptic tubes, American Institution of Chemical Engineers, AIChE Symposium Series, Heat Transfer, 314 (1997) 185 – 190.

[12] R. Liu, A. Fartaj, D. S-K Ting, An experimental study on cross-flow cooling via an elliptical tube array, The 6th ASME-JSME Thermal Engineering Joint Conference, 16-20 March (2003).

[13] H. Brauer, Compact Heat Exchangers, Chemical and Process Engineering, August, (1964) 45–460.

[14] F. J. Schulenberg, Finned elliptical tubes and their application in air-cooled heat exchangers, Journal of Engineering for Industry, Transaction of ASME, Series B, 88 (2) (1966) 179–190.

[15] S. M. Saboya, F. E. M. Saboya, Experiments on elliptic sections in one-and two-row arrangements of plate fin and tube heat exchangers, Experimental Thermal and Fluid Science, 24 (1-2) (2001) 67–75.

[16] J. Y. Jang, J. Y. Yang, Experimental and 3-D numerical analysis of the thermal-hydraulic characteristics of elliptic finned-tube heat exchangers, Heat Transfer Engineering, 19 (4) (1998) 55–67.

[17] A. Hasan, K. Sirén, Performance investigation of plain circular and oval tube evaporatively-cooled heat exchangers, Applied Thermal Engineering, 24 (5-6) (2004) 777–790.

[18] R. C. Pankhurst, D. W. Holder, Wind-tunnel technique: an account of experimental methods in low- and high-speed wind tunnels, London Sir Isaac Pitman (1968).

[19] H. Lassila, Design of smoke wind tunnel, Master degree thesis, Ship and Flight Institute, Helsinki University of Technology, Espoo, Finland (In Finnish) (1974).

[20] A. Zukauskas, Heat transfer from tubes in cross flow, Advances in Heat Transfer, 8 (1972) 93–160.

[21] F. P. Incropera, D. P. DeWitt, Fundamentals of Heat and Mass Transfer, Fourth edition, John Wiley (1996).

[22] V. T. Morgan, The overall convective heat transfer for smooth circular cylinders, Advances in Heat Transfer, 11 (1975) 199–264.

[23] W. G. Vincenti, D. J. Graham, NACA (Nat. Adv. Comm. Aeronaut) Tech. Rep. No. 849. (1946).

[24] E. W. Comings, J. T. Clapp, J. F. Taylor, Air turbulence and transfer processes. Flow normal to cylinders, Ind. Eng. Chem. 40 (1948) 1076–1082.

[25] B. G. van der Hegge Zijnen, Heat transfer from horizontal cylinders to a turbulent air flow, Appl. Sci. Res. Sect. A7 (1957–1958) 205-223.

[26] M. Jacob, Heat transfer, Vol. 1, Wiley, New York (1949).

[27] J. G. Knudsen, D. L. Katz, Fluid Dynamics and Heat Transfer, McGraw-Hill Book Company (1958).

Fig. 1. (a) The tool used to form the oval tubes. (b) Shapes and dimensions of the tested oval tubes.

Fig. 2. Test rig for the thermal measurement.

Fig. 3. (a) Tubes distribution in the test section. (b) Tube passes. (c) Blockage effect on air velocity.

Fig. 4. Method of drag measurement.

Fig. 5. Velocity distribution along the vertical centreline of the wind tunnel outlet.

Fig. 6. Measurement data for the circular tube.

Fig. 7. Thermal measurements for the circular tube and the oval tubes R = 2, 3, and 4 (the error bars are for the circular tube points).

Fig. 8. Thermal measurements for the oval tube R = 3 with the wires, cut-oval tube, and the oval tube R = 3.

Fig. 9. Drag coefficients for the investigated tubes (the error bars are for the circular tube points).

Fig. 10. The combined thermal-hydraulic performance for the tubes (the error bars are for the circular tube points).

Table 1. Average C_d from the measurements and the literature.

Table 2. The average values of the ratio $Nu_D / C_{d\ avg}$ for each oval tube to that for the circular tube.

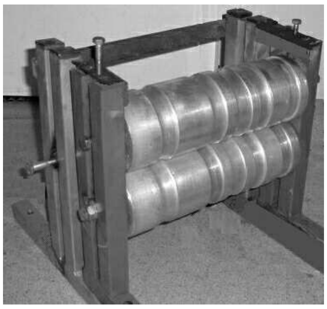

(a)

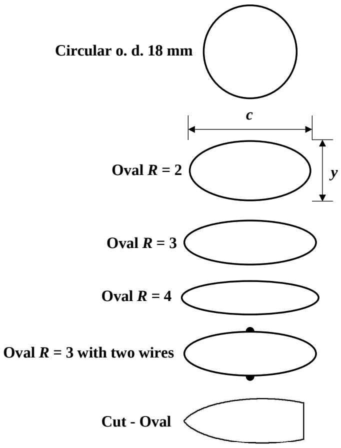

Oval tube	c (mm)	y (mm)	c / y
R = 2	22.2	11.7	1.9
R = 3	24	8.6	2.8
R = 4	25.1	6.3	4
R = 3 with wires	24	8.6	2.8
Cut-oval	23.3	8.6	2.7

(b)

Fig. 1. (a) The tool used to form the oval tubes. (b) Shapes and dimensions of the tested oval tubes.

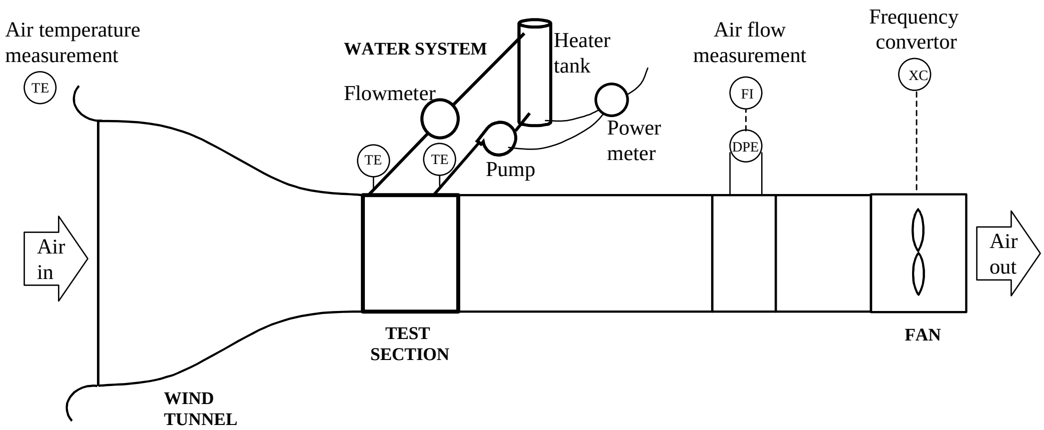

Fig. 2. Test rig for the thermal measurement.

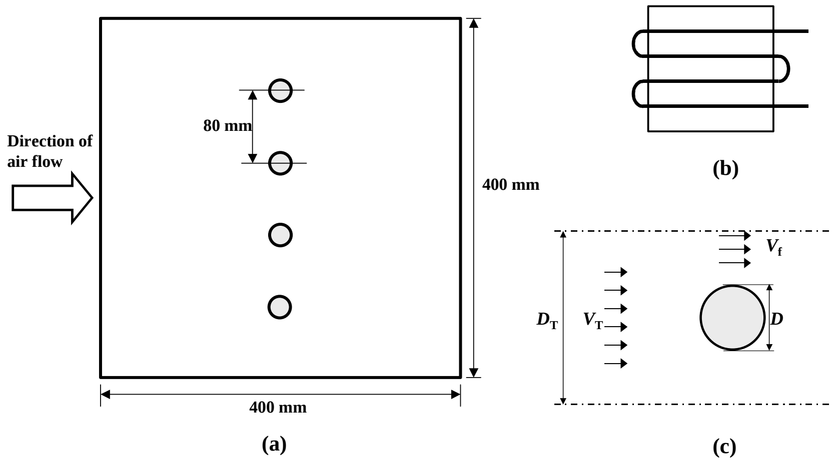

Fig. 3. (a) Tubes distribution in the test section. (b) Tube passes. (c) Blockage effect on air velocity.

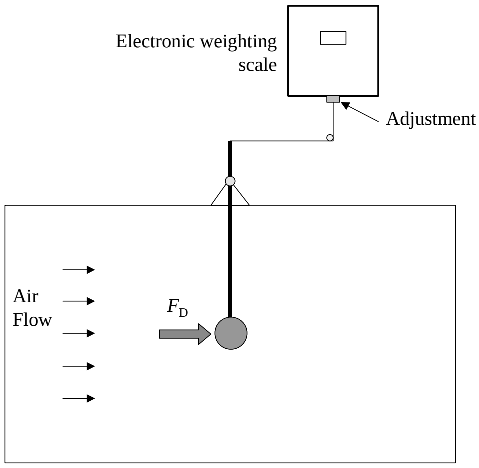

Fig. 4. Method of drag measurement.

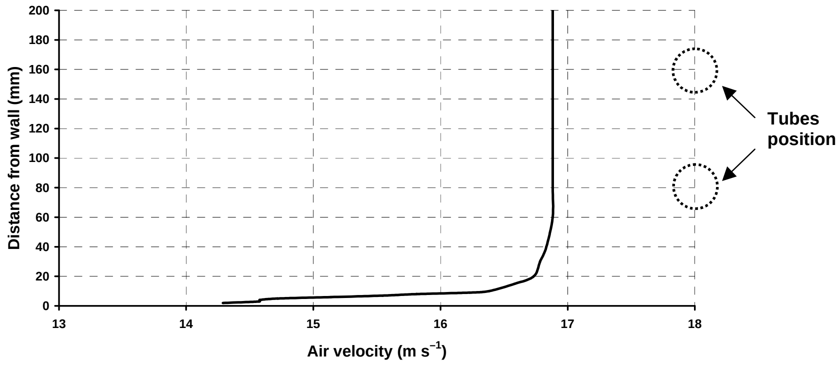

Fig. 5. Velocity distribution along the vertical centreline of the wind tunnel outlet.

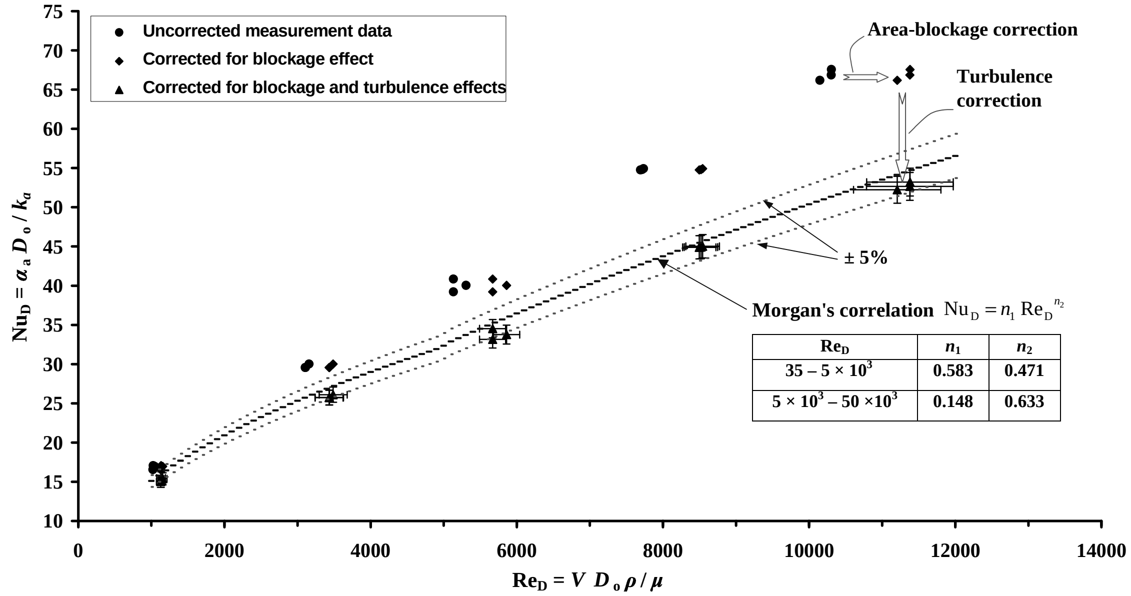

Fig. 6. Measurement data for the circular tube.

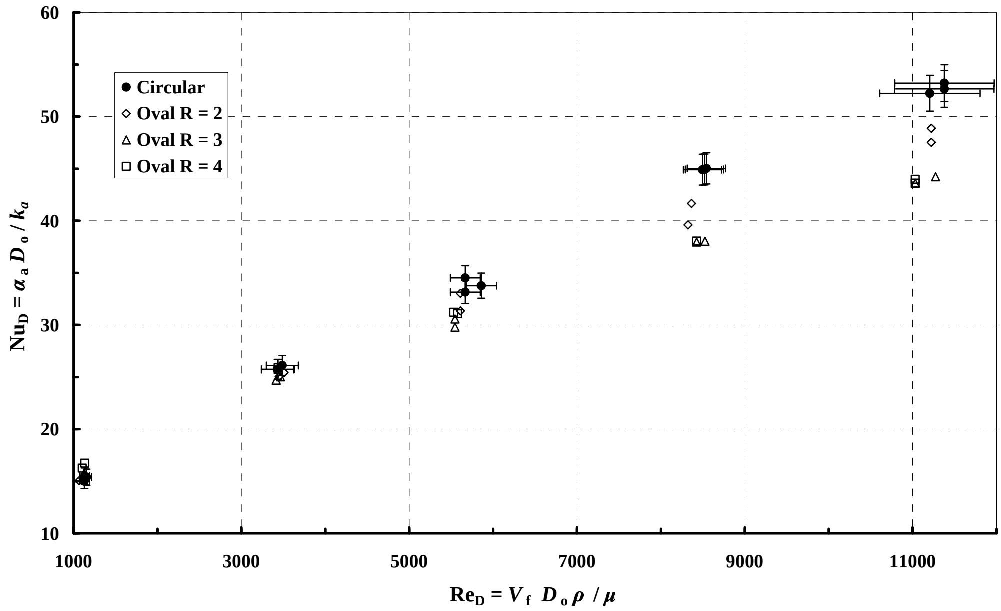

Fig. 7. Thermal measurements for the circular tube and the oval tubes R = 2, 3, and 4 (the error bars are for the circular tube points).

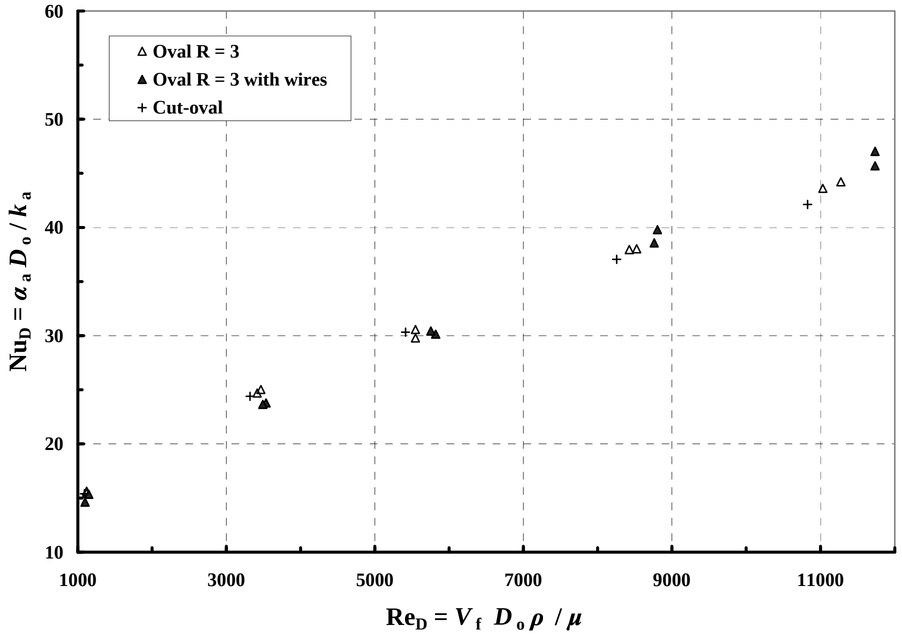

Fig. 8. Thermal measurements for the oval tube R = 3 with the wires, cut-oval tube, and the oval tube R = 3.

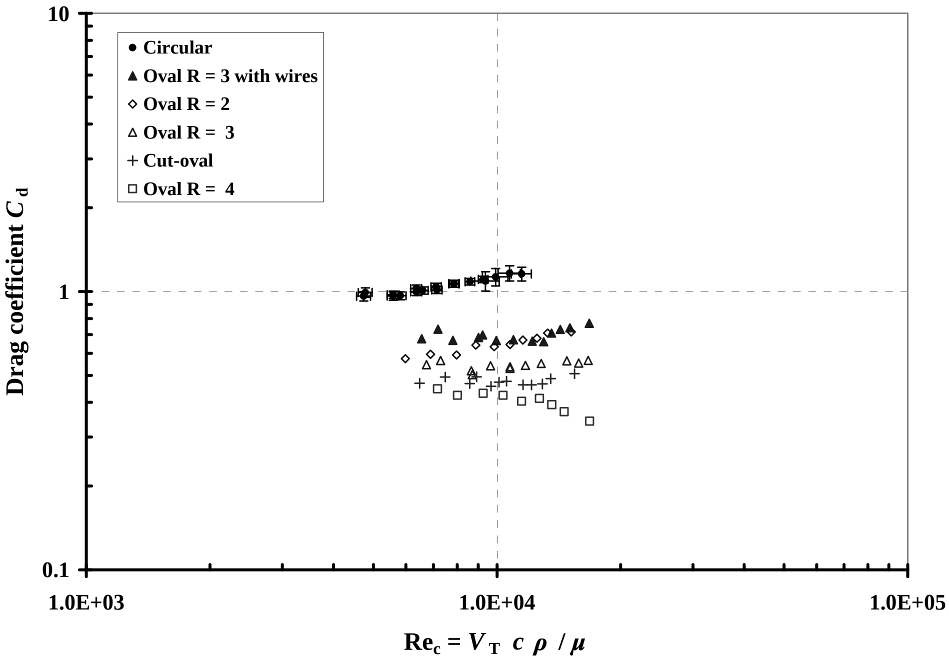

Fig. 9. Drag coefficients for the investigated tubes (the error bars are for the circular tube points).

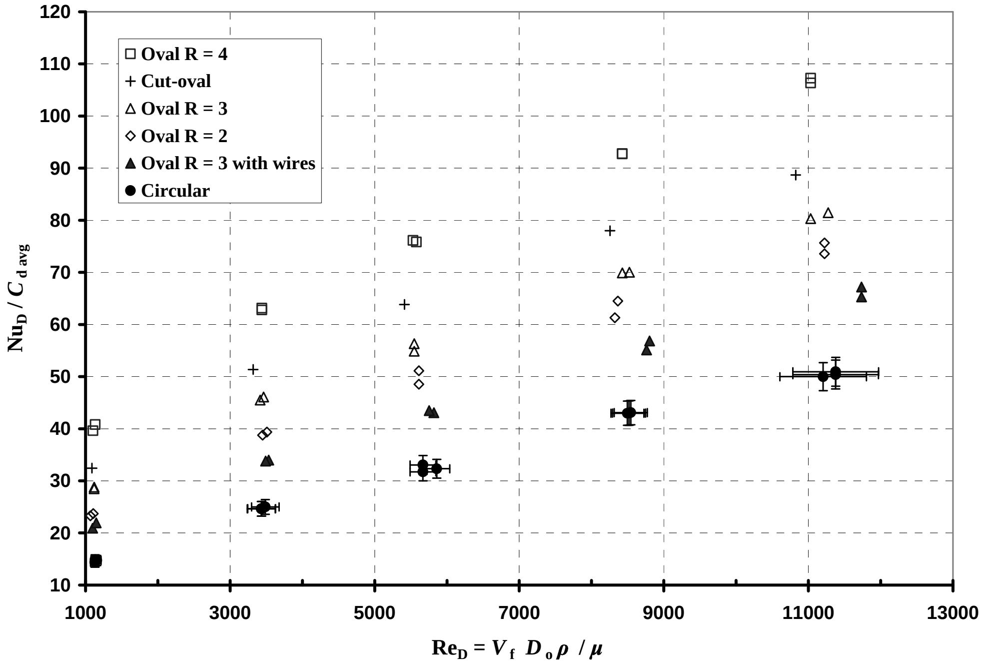

Fig. 10. The combined thermal-hydraulic performance for the tubes (the error bars are for the circular tube points).

Table 1. Average C_d from the measurements and the literature.

$C_{d\ avg}$			
Measured		**Literature**	
Circular	1.05	**Circular**	1 [27], 1.2 [22]
Oval *R* = 2	0.65	**Elliptical *R* = 2**	0.6 [7]
Oval *R* = 3	0.54	**Elliptical *R* = 3**	0.43 [7]
Oval *R* = 4	0.41	**Elliptical *R* = 4**	0.35 [7]
Oval *R* = 3 with wires	0.70	–	–
Cut-oval	0.48	–	–

Table 2. The average values of the ratio $\mathrm{Nu}_\mathrm{D} / C_{\mathrm{d\,avg}}$ for each oval tube to that for the circular tube.

	$\dfrac{(\mathrm{Nu}_\mathrm{D} / C_{\mathrm{d\,avg}})_{\mathrm{oval}}}{(\mathrm{Nu}_\mathrm{D} / C_{\mathrm{d\,avg}})_{\mathrm{circular}}}$
Oval *R* = 2	1.6
Oval *R* = 3	1.8
Oval *R* = 4	2.5
Oval *R* = 3 with wires	1.3
Cut-oval	2.1